

Abiotic and Microbial Oxidation of Laboratory-Produced Black Carbon (Biochar)

ANDREW R. ZIMMERMAN[†]

Department of Geological Sciences, University of Florida,
241 Williamson Hall, P. O. Box 112120, Gainesville,
Florida 32611-2120

Received October 14, 2009. Revised manuscript received
December 12, 2009. Accepted December 15, 2009.

Pyrogenic or “black” carbon is a soil and sediment component that may control pollutant migration. Biochar, black carbon made intentionally by biomass pyrolysis, is increasingly discussed as a possible soil amendment to increase fertility and sequester carbon. Though thought to be extremely refractory, it must degrade at some rate. Better understanding of the rates and factors controlling its remineralization in the environment is needed. Release of CO₂ was measured over 1 year from microbial and sterile incubations of biochars made from a range of biomass types and combustion conditions. Carbon release from abiotic incubations was 50–90% that of microbially inoculated incubations, and both generally decreased with increasing charring temperature. All biochars displayed log–linearly decreasing mineralization rates that, when modeled, were used to calculate 100 year C losses of 3–26% and biochar C half-lives on orders ranging from 10² to 10⁷ years. Because biochar lability was found to be strongly controlled by the relative amount of a more aliphatic and volatile component, measurements of volatile weight content may be a convenient predictor of biochar C longevity. These results are of practical value to those considering biochar as a tool for soil remediation, amelioration, or atmospheric C sequestration.

Introduction

Black carbon (BC) is composed of a continuum of pyrogenic organic materials ranging from slightly charred biomass to charcoal to soot (1). It has received recent attention from environmental chemists for its strong sorption affinity for organic contaminants (2) and for the recent realization that a large portion of the organic carbon found in soils and sediments may be BC (5–40%; e.g., refs 3–6). Thus, BC represents a large, but poorly understood portion of the global carbon that may have served as a carbon sink and oxygen source over geological time scales (7). The intentional production of BC by pyrolysis of biomass yields biochar, which has been suggested as a soil amendment both to improve soil fertility (8) and to sequester atmospheric CO₂ into soils (9). One can envision a “closed-loop” system whereby agricultural or other waste biomass is pyrolyzed to produce bioenergy, and biochar is added back to the soil, aiding the growth of more biomass and yielding “carbon offsets” for the producer or user.

Before we can understand the role BC may have played in past climate changes or how it can be used to mitigate

future climate change, however, we must better understand the stability of BC or biochar in the environment. Because of its highly condensed aromatic structure, its resistance to chemical treatment (e.g., refs 10 and 11) and its occurrence in ancient soils and sediments (e.g., refs 12 and 13); BC has generally been regarded as biologically and chemically recalcitrant (e.g., refs 5, 14, and 15). However, a number of recent observations suggest that, to the contrary, abiotic oxidation of BC occurs and BC can be utilized, at least to some extent, by microbes as a carbon source.

Assuming a BC production rate via natural biomass burning of 0.05–0.3 Gt of C year⁻¹ (7) and a 80 Gt C inventory of BC in soil representing, on average, 5% of the total soil organic matter (1600 Gt of C (16)), an average BC residence time of between 266 and 1600 years (or half-lives of 10²–10³ years) can be calculated, assuming steady-state conditions. It is clear that there must be BC losses; otherwise, soil carbon would be primarily BC (7). Even in the soils of regions of documented repeated fire activity, the quantity of BC calculated to have been produced has not been found (17, 18). Some BC may be lost to erosion, but the pool of BC found in marine sediments is not large enough to balance terrestrial BC production (1). Using ¹⁴C-dating of BC in sediment, BC turnover has been estimated to be in the 1000 year time scale (4), while a soil study comparing fire-affected and fire-protected savannah soils calculated a BC half-life of <100 years (19).

Degradation of BC may occur both abiotically (e.g., chemical oxidation, photooxidation, and solubilization) and biotically (microbial incorporation or oxidative respiration of carbon). A number of studies have claimed that abiotic processes play a major, perhaps even dominant, role in transforming BC. In the presence of oxygen and elevated temperatures (20–22), chemical oxidants (23, 24), ozone (25, 26), or air alone (20, 27–29), the BC surface has been observed to gain O-containing functional groups such as carboxylic acid and become more hydrophilic over time.

Biological utilization of very refractory carbon sources such as charred wood and coal (e.g., refs 30 and 31) and graphite incubated in soils (32) have long been observed. More recently, longer time scale (month to year) laboratory incubations of a number of biochar types have been carried out. Baldock and Smernik (33) found that 20, 13, and 2% of the carbon in red pine wood uncharred or charred at 150 and 350 °C, respectively, was remineralized after 4 months (though this conclusion was based on the insensitive technique of C weight loss). During 60 day microbial incubations, Hamer et al. (34) measured a 0.8, 0.7, and 0.3% loss char BC derived from maize and rye (350 °C, 2 h) and oak (800 °C, 22 h), respectively, as recorded by CO₂ evolution. Incubations of BC mixed with soils have also been carried out with a limited number of biochar types and yielded BC losses of about 0.5 and 3% over 48 days for rye grass and pine (charred briefly in air at 350 °C), respectively (35), and about 4% over 3 years for rye grass charred at 400 °C for 13 h (36).

Because these previous studies were each carried out on a limited number of biochar types, we still have a poor understanding of the natural range of BC lability and how the chemical and physical characteristics of BC control its degradation rate. Here, both abiotic (sterilized) and microbial incubations were carried out on a suite of well-characterized biochars made from a number of parent biomass types and under a range of well-defined combustion conditions. Carbon remineralization was measured monthly as evolved CO₂ over the course of about a year, generating enough detailed data

[†] Corresponding author phone: (352) 392–0070; fax: (352) 392–9294; e-mail: azimmer@ufl.edu.

to construct, for the first time, experimentally based long-term biochar degradation rate models.

Materials and Methods

Biochar Production. Black carbon was produced from six biomass types: the living wood portion of oak (Laurel oak, *Quercus laurifolia*), pine (Loblolly pine, *Pinus taeda*), cedar (Eastern red cedar, *Juniperus virginiana*), and bubinga (the tropical hardwood, *Guibourtia demeusei*), mixed stems and blades of live Eastern gamma grass (*Tripsacum dactyloides*), and sugar cane baggase (sugar cane following industrial processing provided by Florida Crystal Corp.). These materials, all obtained from Florida sources except for bubinga, were dried (60 °C for at least 5 days), cut into 1 cm × 1 cm × 5 cm pieces, and either placed in a thin layer and combusted in an 0.04 m³ oven under full atmosphere (250 °C, chosen to minimize ash formation) or pyrolyzed under N₂ at 400, 525, or 650 °C. For the latter, samples were loosely wrapped in foil in portions of about 4 cm × 4 cm × 10 cm and placed in a 5.5 cm diameter × 50 cm length pipe, which was piped with flowing N₂ (2.3 oven volumes exchanged/min). The temperature routine was 26 °C min⁻¹ heating rate, followed by a 3 h peak temperature hold time and a 3 °C min⁻¹ cooling rate. After cooling, biochars were lightly crushed and sieved into particle size fractions of <0.25 (fine) and 0.25–2 mm (coarse). Additionally, an oak sample and a pine sample were pyrolyzed for peak temperature durations of 72 h.

Biochar Characterization. The biochars produced were chemically and physically examined by a number of methods to investigate the characteristics of BC that may be related to its lability. Specific surface area was determined a Quantachrome Autosorb 1 using both N₂ and CO₂ adsorption for mesopore and micropore surfaces, respectively. Elemental C, N, and H abundances were determined on a Carlo-Erba NA-1500 elemental analyzer, and oxygen content was determined by difference, assuming biochar to be composed of C, N, H, and O only. Volatile matter and ash content (inorganic mass) were determined using a slightly modified ASTM method (D-1762-84) involving measurement of weight loss following combustion of about 10 g of char in a ceramic crucible at 900 °C for 6 min and 750 °C for 6 h, respectively. Volatile C was determined by mass balance following C analysis of the nonvolatile residue. Detailed method descriptions are provided in the Supporting Information.

BC Mineralization Rate. Abiotic and microbial incubations of biochar were carried out in sterilized 12 mL borosilicate vials with rubber septa. For each treatment, six replicate incubations of 20 mg of biochar + 200 mg of cleaned quartz sand + 80 μL of aqueous nutrient solution [60 g of (NH₄)₂SO₄ + 6 g of KH₂PO₄ L⁻¹] were prepared. The sand was added to increase permeability, thus increasing the water and oxygen accessibility for the char. To half of the vials, 20 μL (bringing the incubation to water holding capacity) of sterilized water (abiotic incubation) was added, and to half was added a microbial inoculate, the supernatant of a local forest soil after 24 h shaking in water and centrifugation (biotic incubation). Tubes were incubated in the dark at 32 °C. Oxidation of BC was determined every 2 weeks initially and every 6 weeks after the first 3 months by measuring CO₂ evolution into the vial headspace. Molecular genetic characterization of the microbial inoculate is published elsewhere (37).

Headspace CO₂ was measured by purging for 5 min with CO₂-free air into an automated CO₂ coulometer (UIC Inc., Joliet, IL), leaving the vials refilled with CO₂-free air for reincubation. The analytical detection limit for CO₂, determined using acidification of CaCO₃ standards, was found to be 0.1 μg of C. About every 4 months, 50 μL of sterilized deionized water was added to vials to return samples to about water holding capacity state. For most abiotic and microbial

incubation time periods, variation in C mineralized among replicates was low (standard deviation represented only 13% of the mean, on average, but usually less than 5%). Higher variation often indicated leakage and was corrected by changing the septa in tube caps. Experimental control tubes that were empty or inoculated but contained no char yielded CO₂ measurements of less than 2 μg for any given time period, or the equivalent of 0.1 mg of C/(g of char).

Results

The physical and chemical characteristics of the biochars produced, including their elemental composition and surface area, are provided in Table S1 of the Supporting Information. Time-course plots of cumulative C mineralization and the C mineralization rate for different oak biochars (char weight-normalized, Figure 1a,b and Figure 1c,d, respectively) illustrate trends that were generally observed for all biochar types. First, carbon mineralized from sterilized incubations (abiotic) was always less than or equal to those inoculated with soil microbes (on average, by 41% for oak biochars and 27% overall). Next, the fine biochar (<0.25 mm) grain size fraction released more CO₂ than its corresponding coarse fraction (on average, by 23% for oak biochar and 34% overall for abiotic incubations, and by 22% for oak biochar and 16% overall for microbially inoculated incubations). Lastly, biomass charred at lower temperatures was generally more labile than when charred at higher temperatures. The carbon mineralization rate decreased over the year in both inoculated and abiotic incubations (Figure 1c,d). For both incubation conditions, about half of the C mineralized during 1 year occurred in the first 3–4 months, after which time, mineralization rates were more stable and similar for different biochar types.

So that the lability of different biochar types could be more easily compared, 1 year (exactly) mineralization rates were calculated for all biochars using the slope of the cumulative mineralization versus time curve for the last three data points collected, which was linear in all cases. The results, plotted on both a char weight and C-normalized basis (Figure 2a,b, respectively), show that char lability was controlled more strongly by combustion temperature and duration than by parent biomass type. However, two-way ANOVA analysis (with replication) indicated that both charring temperature and biomass type effects on lability were significant, as was the interaction between these effects.

Compared to lightly charred oak (250 °C under atmosphere, coarse fraction), the C mineralized in 1 year microbial incubations was 27, 43, 44, and 72% less for 400, 525, and 650 °C, and 650 °C at 72 h charred oak, respectively. This pattern of decreasing lability with increasing pyrolysis temperature held for all wood biochars and abiotic incubations as well. However, abiotic and microbial incubations of grass biochar and microbial incubations of sugar cane baggase biochar released the most CO₂ in 1 year when pyrolyzed at 400 °C. A significant direct linear relationship was found between microbial and abiotic C mineralization, both within biomass types (e.g., for oak, $r^2 = 0.86$, $p = 0.01$), and overall, ($r^2 = 0.55$, $p > 0.01$).

Since the C content of these biochars generally increased with charring temperature and duration, the general trend of increasing recalcitrance with increasing charring temperature is even more pronounced when C mineralization is expressed on a C-normalized basis (Figure 2b). Thus, there was a significant negative linear correlation between char C content and cumulative C mineralized in inoculated and abiotic incubations within biomass types such as oak ($r^2 = 0.65$, $p = 0.01$ and $r^2 = 0.65$, $p = 0.02$, respectively) and for chars as a whole ($r^2 = 0.34$, and 0.36, respectively; $p > 0.01$ for both). Figure 2b also depicts the proportion of BC that

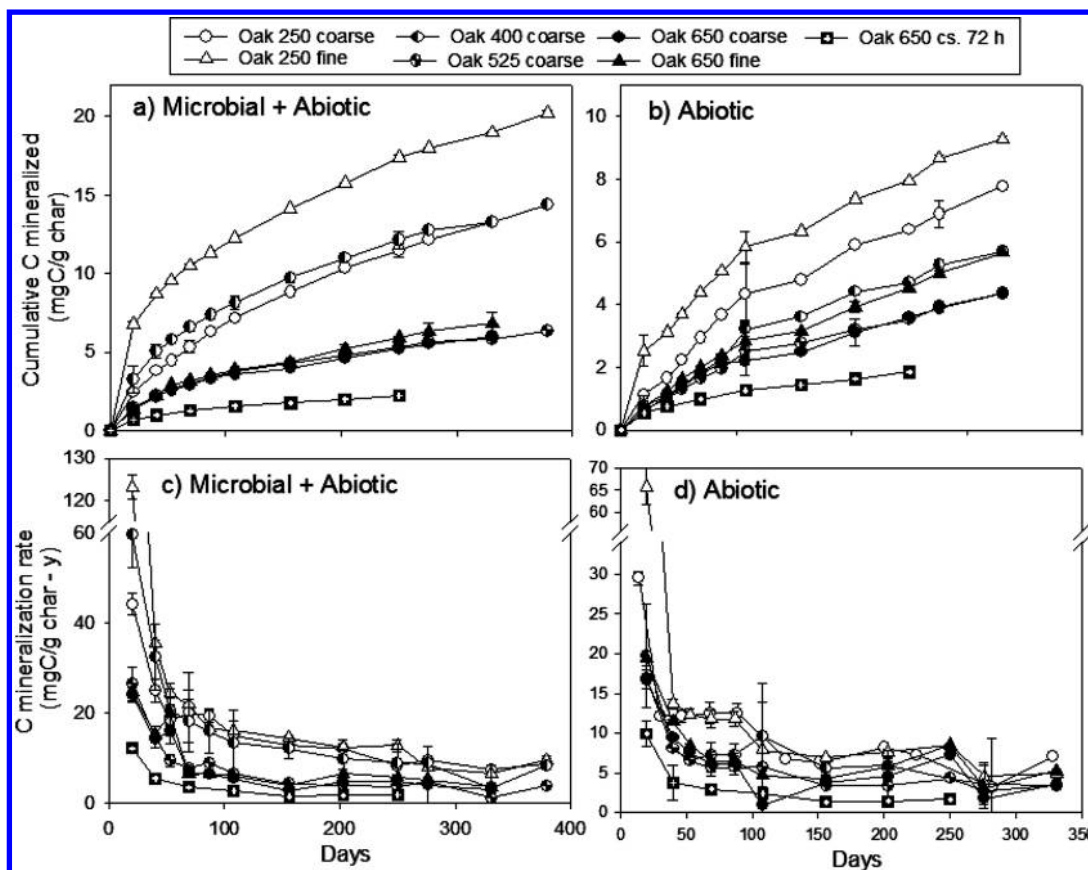


FIGURE 1. Cumulative carbon mineralized (upper panels) and C mineralization rate (lower panels) during 1 year total (microbial + abiotic) and abiotic incubations of oak biochars (all weight-normalized). Note different scales on left axes.

was oxidized during 1 year to have ranged between 0.4 and 3% ($1.4 \pm 0.75\%$ average \pm standard deviation (SD) for inoculated biochar C loss and $1.0 \pm 0.5\%$ for abiotic C loss).

Discussion

The mineralization rates measured in this study are similar to those found in previous studies, though these other studies differed in many details including char type (parent material and charring regime), inoculant, incubation time and temperature, and BC mineralization measurement technique. In addition, the general finding of others of greater biochar stability when charring takes place at greater temperature or over longer time (33, 35, 38) was confirmed. However, in contrast to Hilscher et al. (35), no consistent difference was found between the short-term lability of hardwood, softwood, or grasses. Also, the finding that biotic processes were consistently responsible for about half the BC oxidation during the year contrasted with the findings of Cheng et al. (20) who judged abiotic processes to be more important than biotic ones by examining changes in surficial functional group chemistry following 4-month incubations. It is likely, however, that BC loss via oxidation to CO_2 (mineralization) and the oxidation of the BC surface to O-containing functional groups occur at different rates and by different processes.

Although the abiotic evolution of CO_2 might be attributed to CO_2 desorption from biochar surfaces, this is unlikely because the ratios of abiotic to biotic CO_2 production rate generally increased over the course of the incubations. Abiotic production of CO_2 during humification-type reactions has been shown, such as by the ring cleavage and decarboxylation of catechol (39) and pyrogallol (40). While these reactions were catalyzed by metal oxides, the acidic surface of biochar may have similar catalytic properties toward the oxidation of organic acids and phenols leached from biochar.

The similarities in biochar degradation rate with those in studies in which incubations were carried out in mixtures with soil are somewhat surprising given the probable influence soil would have on moisture and oxygen availability and interactions with minerals and dissolved organic and inorganic ions. Though the stimulatory effect of the presence of labile organic compounds on BC degradation due to co-metabolic “priming” has been shown using additions of glucose (34, 36), the effects of soil humic substances on biochar degradation, and vice versa, is controvertible (41, 42). In any case, this study shows that a labile co-metabolite is not required for microbial utilization of BC. Biochar degradation rates measured in the field may be lower than those measured in the laboratory because of less favorable temperature and moisture conditions in the field, or greater due to the stimulatory effects of bioturbation and the possibility of additional C loss due to photodegradation and BC leaching due to water flow-through.

Biochar Degradation Model. While laboratory-derived degradation rates are, inevitably, made on time scales of a few months or years, longer term estimates of biochar C stability are needed to enable calculations of the effectiveness of biochar amendments as a C sequestration technique and to model the effects of fire on global C cycling. A direct relationship was observed between the logarithmically transformed experimental degradation rate (k in units of year^{-1}) and time (in units of years) data collected over 1 year for both microbial and abiotic incubations. Example least-squares fits are shown in Figure 3, but this relationship was strong for nearly all char types. Linear coefficients of correlation averaged 0.84 ± 0.11 SD ($n = 36$) for microbial and 0.70 ± 0.16 SD for abiotic incubations ($n = 29$) excluding three chars for which $r^2 < 0.4$. Linear parameters for all samples are given in the Supporting Information.

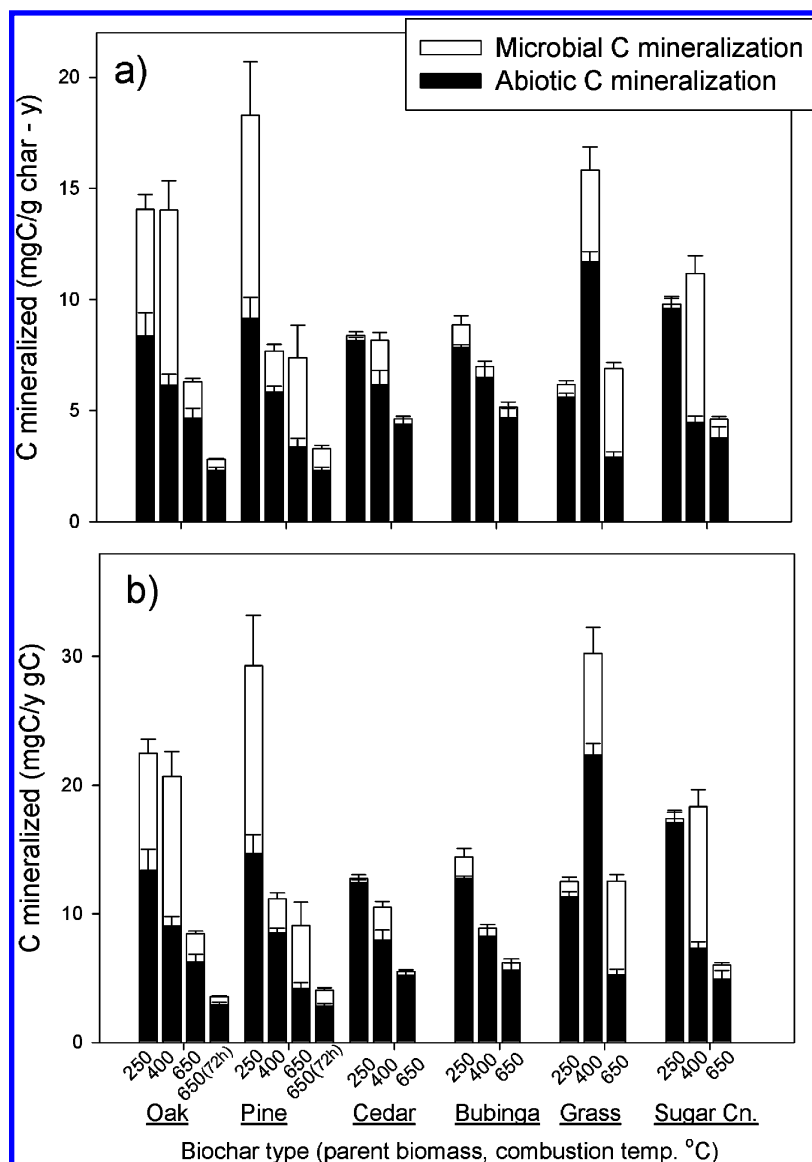


FIGURE 2. Microbially inoculated and abiotic carbon mineralized (a) char weight-normalized and (b) C-normalized) during 1 year incubations of biochars made from different parent biomass types and combustion temperatures (as detailed in text).

Assuming this time-degradation rate relationship is maintained into the future, biochar C loss after any given period of time, t , can be calculated by integrating an equation describing C loss over time, from an initial time, t_0 with the carbon amount C_0 , to a final time t with carbon amount C_t . Thus, with m and b as the slope and intercept, respectively,

$$\frac{dC}{dt} = -C_0 e^b t^m \quad (1)$$

which, after integration can be transformed to

$$C_{\text{lost}} = C_0 - C_t = \left(\frac{C_0 e^b}{m+1} \right) t^{m+1} \quad (2)$$

and the C half-life can be calculated as

$$C_{t_{1/2}} = \left(\frac{m+1}{2e^b} \right)^{1/(m+1)} \quad (3)$$

Results of C half-life and percent C loss after 100 years calculated by this method for biotic incubations of coarse-sized biochars are given in Table 1. Detailed equation derivation steps and alternate solutions for cases where

$m = 1$ and $m < -1$, along with full results for 100 and 1000 years solutions, are given in the Supporting Information. For all incubations, including all biomass types, char temperatures, and particle sizes, the average biochar %C loss after 100 years was 10.3 ± 6.2 SD and 28.4 ± 20.0 SD after 1000 years for microbial incubations. The average long-term %C loss attributable to abiotic processes was quite similar to that derived from the microbial incubations, but the standard deviation was much higher (11.1 ± 10.9 SD after 100 years and 28.8 ± 21.8 SD after 1000 years).

Although the results obtained by this method are quite sensitive to small changes in m and b , so cannot be regarded as hard values, they likely represent, within an order of magnitude, realistic biochar decay characteristics. In addition, they display trends that are generally expected and similar to those observed for 1 year mineralization data. That is, half-life increases drastically with pyrolysis temperature. However, in the long-term modeled results there is a general increase in biochar degradation rate from wood to grass parent materials.

Chemistry and Controls of Biochar Degradation. While the degree to which the biochar degradation rates derived from laboratory incubations are reliable or represent the

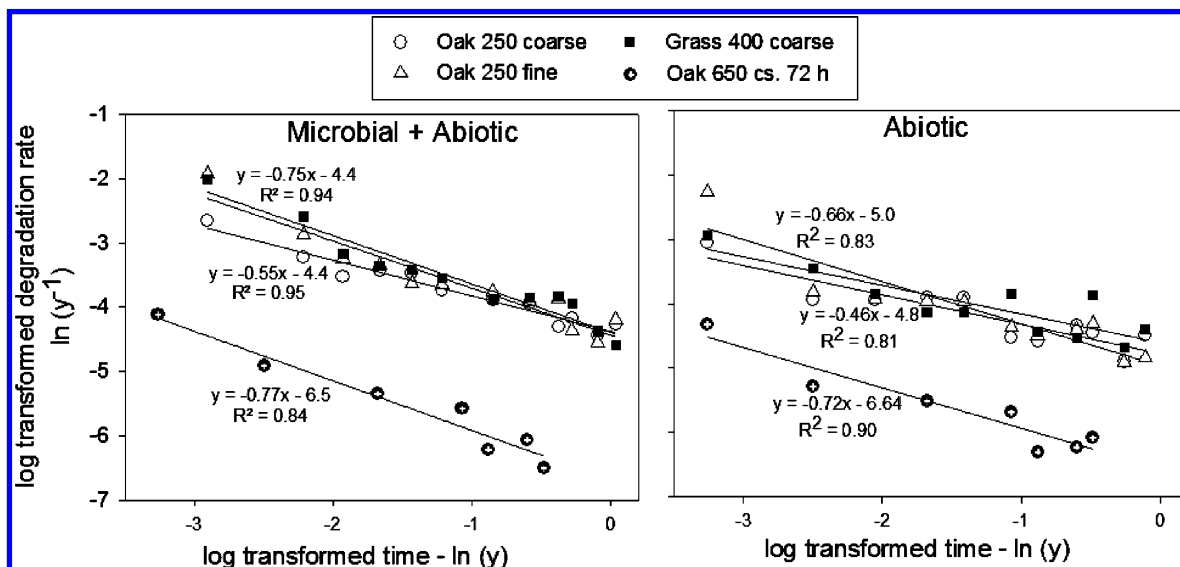


FIGURE 3. Natural log-transformed time versus C mineralization rate during 1 year total (microbial + abiotic) and abiotic incubations of four representative biochars and linear correlations. Degradation rate in units of mg of C (g of char)⁻¹ year⁻¹ was divided by 1000 to yield units of year⁻¹ in which degradation rates are often expressed.

TABLE 1. Modeled Biochar Degradation Parameters (from Abiotic + Biotic Incubations)

parent ^a	250 °C		400 °C		525 °C		650 °C		72 h at 650 °C	
	t _{1/2} ^b (y)	C _{lost 100years} (%)	t _{1/2} (y)	C _{lost 100years} (%)	t _{1/2} (y)	C _{lost 100years} (%)	t _{1/2} (y)	C _{lost 100years} (%)	t _{1/2} (y)	C _{lost 100years} (%)
oak	840	20	1020	18	9590	7	96200	6	4.0 × 10 ⁷	1.9
pine	c	7	990	14	6790	8	17000	6	71800	3.2
cedar	730	16	23800	7	12800	7	2.0 × 10 ⁷	3	nd	nd
Bubinga	1200	15	4300	8	nd ^d	nd	15600	6	nd	nd
gamma grass	260	26	370	27	930	17	150 ^e	37	nd	nd
sugar cane	690	17	9310	11	2280	12	146600	4	nd	nd

^a All data are for coarse (0.25–2 mm) size fraction, 3 h at peak temperature except where indicated. ^b Biochar carbon half-life. ^c Cannot be calculated. ^d nd = not determined. ^e Not reliable since $r^2 < 0.4$.

actual rate of BC loss in soil or sediments can be argued, these findings and the theoretical model developed here provide insight into the chemical nature of biochar and the controls on its lability. The stability of organic matter in the environment is generally thought to be controlled by both its degree of protection by physical structures from microbially produced exoenzymes and to its inherent chemical recalcitrance (e.g., ref 43). There is contradictory evidence as to the importance of the former mechanism, via aggregate formation, for BC in soil (44, 45). In any case, physical protection imparted by associated minerals cannot account for variations in BC lability in this study which used biochar and quartz sand alone. However, our finding that biochar of finer particle size mineralized C at greater rates than their corresponding coarse fraction, even though the fine and coarse fractions had similar N₂-BET surface areas (data not shown), indicates that intrasurface accessibility may be a controlling factor. For biotic incubations, it may be that extracellular enzymes are size-excluded or sterically hindered from much of the BC surface, whereas, for abiotic incubations, a diffusional limitation of some reactant such as water or oxygen to internal surfaces may be invoked.

A conceptual model of recently produced biochar degradation has been presented in which biochar is generalized to be biphasic, containing a labile and a stable pool of carbon (46). The chemical character of these two pools are as follows: (1) an aliphatic portion that is more readily remineralized and is in less abundance for biochar produced at higher temperatures and (2) an aromatic portion that is oxidized more slowly (perhaps mainly abiotically), forming surficial, oxygen-containing functional groups including carboxylic

acids. Elemental signatures and NMR and FT-IR spectroscopy have detected the disappearance of aliphatic C and increase in aromatic C (and O-aryl C) that occurs with increased pyrolysis temperature (33, 35), and the consumption of aliphatic C and production of carboxyl/carbonyl C following incubation (20, 35).

Further insight into the controls on BC degradation can be gained through an examination of the relationships between degradation parameters (both measured and modeled C loss) and the physical and chemical characteristic of biochar (Tables S1 and S2 and Figure S1 in the Supporting Information). The strongest linear relationship was found between measures of C lability such as measured total and abiotic 1 year C loss or modeled 100 year %C lost and biochar volatile weight content ($r^2 = 0.35$ – 0.44 , all $p < 0.01$). Strong indirect relationships were also found between these measures of biochar lability and both mesopore and micropore surface area (measured by N₂ and CO₂ adsorption, respectively) with r^2 ranging from 0.18 to 0.49. Biochar lability was also directly related to oxygen content and indirectly to C content but was only weakly related to volatile C content. These relationships suggest a biphasic biochar composition consisting of a more labile volatile component of relatively lower C and higher oxygen content (relatively aliphatic) and a nonvolatile, high C and low O material (relatively aromatic). The former may primarily occur within pores made up of a lattice of the latter material, as suggested by the rapid increase in surface area that occurs with higher pyrolysis temperatures.

However, the mathematical model developed here to fit the biochar incubation data implies that BC loss rates are not biphasic but, rather, vary along a continuum from more labile

to extremely refractory. A similar model, the so-called “power-model” has been used to describe the log–log relationship between degradation rate and time of burial of a mixture of organic matter types in a sediment core (47). Reactivity continuously and exponentially decreases as more labile or, perhaps, more physically accessible organic compounds oxidize, leaving behind a progressively more refractory or more physically inaccessible residue. In a sample of biochar, the C that is lost first is most likely to be aliphatic and closer to a particle’s external surfaces, and residual C is more likely to be either part of highly condensed aromatic structures or condensates within protective internal pores that are more abundant in higher temperature biochars. The greater degradation rate of the biochar samples of finer particle size attests to the additional importance of physical protection in controlling BC degradation.

For the purposes of those planning C sequestration projects or assigning C credits for biochar burial, volatile content appears to be the most convenient method for estimating biochar C longevity. A figure and equation describing the linear relationship between biochar C loss after 100 years and volatile carbon content is provided in the Supporting Information. However, experiments assessing the role of the soil environment, including temperature and moisture, are needed to better predict biochar C sequestration.

Acknowledgments

I thank Dr. Mark Panning (Department of Geological Sciences, University of Florida) for his generous help with mathematical solutions and Dr. Jason Curtis and Atanu Mukherjee for assistance with chemical analyses. This work was supported by NSF-EAR Grant No. 0819706, the Geobiology and Low Temperature Geochemistry Program.

Supporting Information Available

Additional details on the materials and methods used, detailed mathematical derivation of the model equations, and full tabulated experimental and model results. This material is available free of charge via the Internet at <http://pubs.acs.org>.

Literature Cited

- Masiello, C. A. New directions in black carbon organic geochemistry. *Mar. Chem.* **2004**, *92* (1–4), 201–213.
- Cornelissen, G.; Gustafsson, O.; Bucheli, T. D.; Jonker, M. T. O.; Koelmans, A. A.; Van Noort, P. C. M. Extensive sorption of organic compounds to black carbon, coal, and kerogen in sediments and soils: Mechanisms and consequences for distribution, bioaccumulation, and biodegradation. *Environ. Sci. Technol.* **2005**, *39*, 6881–6895.
- Song, J.; Peng, P. A.; Huang, W. Black carbon and kerogen in soils and sediments. 1. Quantification and characterization. *Environ. Sci. Technol. Lett.* **2003**, *30* (4), 1185.
- Masiello, C. A.; Druffel, E. R. M. Organic and black carbon C-13 and C-14 through the Santa Monica Basin sediment oxic-anoxic transition. *Geophys. Res. Lett.* **2003**, *30* (4), 1185.
- Skjemstad, J. O.; Reicosky, D. C.; Wilts, A. R.; McGowan, J. A. Charcoal carbon in US agricultural soils. *Soil Sci. Soc. Am. J.* **2002**, *66* (4), 1249–1255.
- Schmidt, M. W. I.; Skjemstad, J. O.; Czimczik, C. I.; Glaser, B.; Prentice, K. M.; Gelin, Y.; Kuhlbusch, T. A. Comparative analysis of black carbon in soils. *Global Biogeochem. Cycles* **2001**, *15* (1), 163–167.
- Kuhlbusch, T. A.; Crutzen, P. J. Toward a global estimate of black carbon in residues of vegetation fires representing a sink of atmospheric CO₂ and a source of O₂. *Global Biogeochem. Cycles* **1995**, *9* (4), 491–501.
- Glaser, B.; Lehmann, J.; Zech, W. Ameliorating physical and chemical properties of highly weathered soils in the tropics with charcoal—A review. *Biol. Fert. Soils* **2002**, *35* (4), 219–230.
- Lehmann, J. A handful of carbon. *Nature* **2007**, *447* (7141), 143–144.
- Skjemstad, J. O.; Clarke, P.; Taylor, J. A.; Oades, J. M.; McClyure, S. G. The chemistry and nature of protected carbon in soil. *Aust. J. Soil Res.* **1996**, *34*, 251–271.
- Glaser, B.; Haumaier, L.; Guggenberger, G.; Zech, W. Black carbon in soils: The use of benzenecarboxylic acid as specific markers. *Org. Geochem.* **1998**, *29* (4), 811–819.
- Pessenda, L. C. R.; Ledru, M. P.; Gouveia, S. E. M.; Aravena, R.; Ribeiro, A. S.; Bendassolli, J. A.; Boulet, R. Holocene palaeoenvironmental reconstruction in northeastern Brazil inferred from pollen, charcoal and carbon isotope records. *Holocene* **2005**, *15* (6), 812–820.
- Schmidt, M. W. I.; Noack, A. G. Black carbon in soils and sediments: Analysis, distribution, implications, and current challenges. *Global Biogeochem. Cycles* **2000**, *14* (3), 777–793.
- Seiler, W.; Crutzen, P. J. Estimates of gross and net fluxes of carbon between the biosphere and the atmosphere from biomass burning. *Climatic Change* **1980**, *2* (3), 207–247.
- Kuhlbusch, T. A. J. Black carbon and the global carbon cycle. *Science* **1998**, *280*, 1903–1904.
- Eswaran, H.; Van Den Berg, E.; Reich, P. Organic carbon in soils of the world. *Soil Sci. Soc. Am. J.* **1993**, *57* (1), 192–194.
- Ohlson, M.; Tryterud, E. Interpretation of the charcoal record in forest soils: forest fires and their production and deposition of macroscopic charcoal. *Holocene* **2000**, *10* (4), 519–525.
- Czimczik, C. I.; Preston, C. M.; Schmidt, M. W. I.; Schulze, E. D. How surface fire in Siberian Scots pine forests affects soil organic carbon in the forest floor: Stocks, molecular structure, and conversion to black carbon (charcoal). *Global Biogeochem. Cycles* **2003**, *17* (1), 20.1–20.14.
- Bird, M. I.; Moyo, C.; Veenendaal, E. M.; Lloyd, J.; Frost, P. Stability of elemental carbon in a savanna soil. *Global Biogeochem. Cycles* **1999**, *13* (4), 923–932.
- Cheng, C. H.; Lehmann, J.; Thies, J. E.; Burton, S. D.; Engelhard, M. H. Oxidation of black carbon by biotic and abiotic processes. *Org. Geochem.* **2006**, *37* (11), 1477–1488.
- Morterra, C.; Low, M. J. D.; Severdia, A. G. IR studies of carbons. 3. The oxidation of cellulose chars. *Carbon* **1984**, *22* (1), 5–12.
- Toles, C. A.; Marshall, W. E.; Johns, M. M. Surface functional groups on acid-activated nutshell carbons. *Carbon* **1999**, *37* (8), 1207–1214.
- Moreno-Castilla, C.; Lopez-Ramon, M. V.; Carrasco-Marín, F. Changes in surface chemistry of activated carbons by wet oxidation. *Carbon* **2000**, *38* (14), 1995–2001.
- Puri, B. R.; Sharma, S. K. Studies in formation and properties of carbon-oxygen surface complexes. 2. Nature of surface complexes formed on progressive treatment with oxidising solutions. *J. Indian Chem. Soc.* **1968**, *45* (12), 1115–8.
- Kawamoto, K.; Ishimaru, K.; Imamura, Y. Reactivity of wood charcoal with ozone. *J. Wood Sci.* **2005**, *51* (1), 66–72.
- Sergides, C. A.; Jassim, J. A.; Chughtai, A. R.; Smith, D. M. The structure of hexane soot. 3. Ozonation studies. *Appl. Spectrosc.* **1987**, *41* (3), 482–492.
- Billinge, B. H. M.; Evans, M. G. The growth of surface oxygen complexes on the surface of activated carbon exposed to moist air and their effect on methyl iodide-131 retention. *J. Chim. Phys. Phys.-Chim. Biol.* **1984**, *81* (11–1), 779–784.
- Adams, L. B.; Hall, C. R.; Holmes, R. J.; Newton, R. A. An examination of how exposure to humid air can result in changes in the adsorption properties of activated carbons. *Carbon* **1988**, *26* (4), 451–459.
- Cohen-Ofri, I.; Popovitz-Biro, R.; Weiner, S. Structural characterization of modern and fossilized charcoal produced in natural fires as determined by using electron energy loss spectroscopy. *Chem.—Eur. J.* **2007**, *13* (8), 2306–2310.
- Potter, M. C. Bacteria as agents in the oxidation of amorphous carbon. *Proc. R. Soc. London, Ser. B* **1908**, *80* (539), 239–259.
- Scott, C. D.; Strandberg, G. W.; Lewis, S. N. Microbial solubilization of coal. *Biotechnol. Prog.* **1986**, *2*, 131–139.
- Shneour, E. A. Oxidation of graphitic carbon in certain soils. *Science* **1966**, *151* (3713), 991–8.
- Baldock, J. A.; Smernik, R. J. Chemical composition and bioavailability of thermally altered *Pinus resinosa* (Red Pine) wood. *Org. Geochem.* **2002**, *33* (9), 1093–1109.
- Hamer, U.; Marschner, B.; Brodowski, S.; Amelung, W. Interactive priming of black carbon and glucose mineralisation. *Org. Geochem.* **2004**, *35*, 823–830.
- Hilscher, A.; Heister, K.; Siewert, C.; Knicker, H. Mineralisation and structural changes during the initial phase of microbial degradation of pyrogenic plant residues in soil. *Org. Geochem.* **2009**, *40* (3), 332–342.

- (36) Kuzyakov, Y.; Subbotina, I.; Chen, H. Q.; Bogomolova, I.; Xu, X. L. Black carbon decomposition and incorporation into soil microbial biomass estimated by C-14 labeling. *Soil Biol. Biochem.* **2009**, *41* (2), 210–219.
- (37) Khodadad, C. L. M.; Zimmerman, A. R.; Uthandi, S.; Foster, J. S. Changes in microbial community composition in soils amended with pyrogenic carbon. *Appl. Environ. Microb.*, submitted for publication.
- (38) Bruun, S.; Jensen, E. S.; Jensen, L. S. Microbial mineralization and assimilation of black carbon: Dependency on degree of thermal alteration. *Org. Geochem.* **2008**, *39* (7), 839–845.
- (39) Majcher, E. H.; Chorover, J.; Bollag, J. M.; Huang, P. M. Evolution of CO₂ during birnessite-induced oxidation of C-14-labeled catechol. *Soil Sci. Soc. Am. J.* **2000**, *64* (1), 157–163.
- (40) Wang, M. C.; Huang, P. M. Ring cleavage and oxidative transformation of pyrogallol catalyzed by Mn, Fe, Al, and Si oxides. *Soil Sci.* **2000**, *165* (12), 934–942.
- (41) Lehmann, J.; Sohi, S. Comment on “fire-derived charcoal causes loss of forest humus”. *Science* **2008**, *321*, 5894.
- (42) Wardle, D. A.; Nilsson, M. C.; Zackrisson, O. Fire-derived charcoal causes loss of forest humus. *Science* **2008**, *320* (5876), 629–629.
- (43) Sollins, P.; Homann, P.; Caldwell, B. A. Stabilization and destabilization of soils organic matter: Mechanisms and controls. *Geoderma* **1996**, *74*, 65–105.
- (44) Brodowski, S.; John, B.; Flessa, H.; Amelung, W. Aggregate-occluded black carbon in soil. *Eur. J. Soil Sci.* **2006**, *57* (4), 539–546.
- (45) Liang, B.; Lehmann, J.; Solomon, D.; Sohi, S.; Thies, J. E.; Skjemstad, J. O.; Luizao, F. J.; Engelhard, M. H.; Neves, E. G.; Wirrick, S. Stability of biomass-derived black carbon in soils. *Geochim. Cosmochim. Acta* **2008**, *72* (24), 6069–6078.
- (46) Lehmann, J.; Czimczik, C.; Laird, D.; Sohi, S. Stability of biochar in the soil. In *Biochar for Environmental Management: Science and Technology*, Lehmann, J., Joseph, S., Eds. Earthscan: London, 2009; pp 183–205.
- (47) Middleburg, J. J. A simple rate model for organic matter decomposition in marine sediments. *Geochim. Cosmochim. Acta* **1989**, *53*, 1577–1581.

ES903140C

Supporting Information Section

Title: Abiotic and microbial oxidation of laboratory-produced black carbon (biochar)

Author: Andrew R. Zimmerman, University of Florida, Department of Geological Sciences

Journal: Environmental Science & Technology

Prepared: December 10, 2009

15 pages

1 figure

6 tables

Additional Method Information

Specific Surface Area was determined using both N₂ and CO₂ adsorption on a Quantachrome Autosorb 1. External surface area, which includes pores >1.5 nm was calculated using multi-point adsorption data from the linear segment (in partial pressure range of 0.001 to 0.03) of the N₂ adsorption isotherms (at 77 K) using Brunauer-Emmett-Teller (BET: Brunauer et al., 1938) theory. Pore size distributions were calculated from desorption branch isotherms using the Barrett-Joyner-Halenda (BJH) theory (Barrett et al., 1951). Internal surface area and pore volume for pores <1.5 nm were determined using CO₂ adsorption isotherms (at 273 K) generated in the partial pressure range <0.02. These isotherms, which constitute the so-called kernel, are interpreted using Grand Canonical Monte Carlo (GCMC) simulations or the Non-Local Density Functional Theory (NLDFT). All BC samples were de-gassed under vacuum at 200°C for at least 24 hours prior to analysis.

Elemental C, N and H abundances were determined on a Carlo-Erba NA-1500 CNS Elemental Analyzer. After grinding in a silica mortar and pestle, biochar amounts of about 6 mg for H and N and about 0.5 mg for C were weighed into tin capsules. Samples were flash-combusted in a quartz column containing chromium oxide and silvered cobaltous/cobaltic oxide at 1000°C in an oxygen-rich atmosphere. The sample gas is then carried in a He carrier stream through a hot reduction column (650°C) consisting of reduced elemental copper to remove oxygen and convert NO_x to N₂. The effluent stream then passes through a chemical (magnesium perchlorate) trap to remove water. The stream then passes through a 1.5 meter gas chromatographic column at 55°C that separates the N₂, H₂ and CO₂ gases before detection by thermal conductivity. Oxygen content was calculated by difference assuming a composition of C, N, H, and O, only. This assumption could have led to an over-estimate of oxygen content. If ash content (below) is assumed to represent inorganic elemental weight %, oxygen weight% can be re-calculated as 1-10% less for most samples. For Oak650, for an ash content of 3.7%, oxygen weight% would be 20.4% less and the grasses, with ash contents ranging 7-25% would have re-calculated oxygen weight% that are 16-50% less.

Volatile matter and ash content was determined using a slightly modified version of ASTM method (D-1762-84). About 10 mg of non-ground biochar that had been kept in a drying oven for at least 2 hrs at 100°C and allowed to cool in a desiccator was weighed into pre-weighed

ceramic crucibles. Volatile matter content was determined as weight loss after combustion with a loose ceramic cap at 850-900°C for 6 min. (set-point was 900°C but some cooling occurred while oven door was open). Ash content was determined as weight loss after combustion at 750°C for 6 h with no ceramic cap. Sample weight was taken after cooling in a desiccator for 1 h. Volatile C was determined by mass balance following analysis of the C content of the ground non-volatile residue (as above).

Solution for biochar degradation equation

NOTE: This solution can be applied only when the slope, $m > -1$ because of mathematical restrictions.

Using the equation for first order degradation, change in amount of carbon, C , over time, t is:

$$\frac{dC}{dt} = -C_0 k \quad (1)$$

where C_0 is the initial C present and k is the apparent degradation rate constant.

Also, k was found to vary with time such that:

$$\ln(-k) = m \ln(t) + b \quad (2)$$

where m is slope and b is the intercept when fitted to a line using least squares technique.

Re-arranging eq. 2,

$$-k = e^{b} t^m \quad (3)$$

and substituting eq. 3 into eq. 1 yields:

$$\frac{dC}{dt} = -C_0 e^{b} t^m \quad (4)$$

Now, integrating eq. 4 from time = 0 to time t , yields:

$$C_t = \left(\frac{C_0 e^b}{m+1}\right) t^{m+1} + K \quad (5)$$

where C_t is carbon present at time t and K is the integration constant.

When $t = 0$, $C_0 = K$, so C lost at any time t can be written as:

$$C_{\text{lost}} = C_0 - C_t = \left(\frac{C_0 e^b}{m+1}\right) t^{m+1} \quad (6)$$

To calculate biochar C half-life

At the C half-life:

$$C_{t_{1/2}} = \frac{C_t}{C_0} = \frac{1}{2} \quad \text{or} \quad C_t = \frac{C_0}{2} \quad (7)$$

Re-arranging eq. 6:

$$C_t = C_o \left(1 - \frac{C_o e^b}{m+1} t^{m+1}\right) \quad (8)$$

Substituting eq. 7 into eq. 8 and re-arranging:

$$C_{t_{1/2}} = \left(\frac{m+1}{2e^b}\right)^{\frac{1}{m+1}} \quad (9)$$

Alternate solution for biochar C loss equation

NOTE: When $m < -1$, the above equation is not solvable so it is necessary to integrate choosing the initial time, t_o , to be something greater than zero (0.01 y, for example). One can view this as necessary, in physical terms, because the equation predicts physically unreasonable large decay rates at times approaching zero. However, still, a carbon half life cannot be calculated because degradation rate diminishes so rapidly that the amount of carbon remaining, C_t , becomes asymptotic with some value of carbon greater than half the initial amount.

Integrating eq. 4 (above) from a time of t_o to t yields:

$$C_t = \left(\frac{C_o e^b}{m+1}\right)t^{m+1} + \left(\frac{C_o e^b}{m+1}\right)t_o^{m+1} + C_o \quad (10)$$

So C lost at any time, t , can be written as:

$$C_{\text{lost}} = C_o - C_t = \left(\frac{C_o e^b}{m+1}\right)(t^{m+1} - t_o^{m+1}) \quad (11)$$

Alternate solution for biochar C loss equation for special case of when $m = -1$

When $m = -1$, can integrate eq. 4 from time = 1 to t .

$$C_t = -C_o e^b \ln(t) + C_o \quad (12)$$

Then C lost is:

$$C_{\text{loss}} = C_o e^b \ln(t) \quad (13)$$

Table S1. Chemical and physical characteristics of biochars

Biomass/Char T ¹	OC ² (wt.%)	O% (wt.%)	Yield (wt.%)	Volatile (wt.%)	Volatile C (wt.%)	Ash (wt.%)	S.A.-N ₂ (m ² /g)	S.A.-CO ₂ (m ² /g)
Bubinga (parent)	46.1							
Bubinga 250	61.5	34.9	52.5	66.4	32.6	0.9	5.4	262.5
Bubinga 400	78.6	17.6	33.2	41.1	28.7	1.8	6.1	428.8
Bubinga 525	85.3	11.4	28.5	35.0	27.0	1.2	500.9	613.1
Bubinga 650	83.0	13.8	29.3	22.3	15.8	1.3	548.9	627.1
Cedar (parent)	47.1							
Cedar 250	65.6	31.4	24.6	62.6	34.2	0.9	68.1	522.2
Cedar 400	77.8	17.9	35.3	52.0	37.0	0.4	7.2	354.1
Cedar 525	85.4	11.3	30.3	39.1	33.0	1.3	386.5	598.1
Cedar 650	84.2	11.4	29.5	30.9	23.8	1.0	490.1	607.0
G. Grass (parent)	41.0							
G. Grass 250	52.7	42.5	52.2	62.5	28.6	6.8	4.1	146.0
G. Grass 400	58.6	35.4	65.5	51.4	29.6	13.2	12.9	129.0
G. Grass 525	55.0	40.6	40.9	36.7	23.9	24.8	31.5	335.1
G. Grass 650	63.8	31.8	34.6	33.0	20.6	15.9	425.9	345.0
L. Oak (parent)	44.5							
L. Oak 250	55.2	41.5	44.1	66.0	27.0	1.4	1.8	270.1
L. Oak 400	69.6	25.9	46.9	51.9	30.6	2.6	2.2	176.0
L. Oak 525	75.1	21.7	29.2	36.4	22.0	6.8	38.2	525.4
L. Oak 650	78.8	18.2	32.1	20.7	15.1	3.7	218.7	486.9
L. Pine (parent)	45.4							
L. Pine 250	58.0	38.2	28.4	61.1	25.0	0.3	139.7	501.2
L. Pine 400	68.6	25.9	41.3	58.6	33.3	0.5	2.9	410.8
L. Pine 525	80.6	14.0	37.8	25.7	14.6	1.2	206.1	396.4
L. Pine 650	83.0	12.2	26.6	25.2	16.5	1.1	393.9	585.7
Sug. Cn. Bag. (parent)	45.2							
Sug. Cn. Bag. 250	56.2	40.4	32.8	71.8	36.9	9.5	24.3	334.9
Sug. Cn. Bag. 400	60.9	33.7	26.1	63.9	32.8	2.7	6.4	204.4
Sug. Cn. Bag. 525	65.7	30.2	20.7	55.1	31.4	8.7	416.3	523.1
Sug. Cn. Bag. 650	72.0	24.0	37.1	48.8	33.4	6.8	116.6	576.0
L. Oak 400_72hrs	63.2	31.8	43.6	41.9	16.0	5.2	2.3	nd
L. Oak 650_72hrs	77.3	20.1	28.5	14.7	5.4	7.4	505.0	nd
L. Pine 400_72hrs	72.1	22.3	37.3	51.2	32.6	0.9	4.9	289.2
L. Pine 650_72hrs	82.5	14.2	27.2	21.7	19.8	1.2	416.4	640.9

1. Additional details on plant type described in text. Peak temperature of combustion held at 3 h unless specified otherwise

2. OC = organic carbon content, O is oxygen content, yield = weight biochar/parent biomass, volatile is mass volatilized after 6 min at 900 C, ash is residual weight after combustion at 750 C for 6 h, S.A.-N₂ and S.A.-CO₂ is surface area determined by N₂ and CO₂ adsorption, respectively, nd = not determined.

Table S2. Microbially inoculated and abiotic carbon mineralized during one year incubations (char weight-normalized: mg g^{-1}) of biochars made from different parent biomass types and combustion temperatures (as shown in Figure 2 or manuscript).

	250 °C		400 °C		525 °C		650 °C		72 hr @ 650 °C	
	biotic	abiotic	biotic	abiotic	biotic	abiotic	biotic	abiotic	biotic	abiotic
Parent										
Oak	14.1 ± 0.7	8.4 ± 1	14 ± 1.3	6.1 ± 0.5	6.2 ± 0.3	4.7 ± 0.8	6.3 ± 0.2	4.7 ± 0.5	2.8 ± 0.1	2.3 ± 0.2
Pine	18.0 ± 2.4	9.2 ± 0.9	7.7 ± 0.3	5.9 ± 0.2	4.4 ± 0.4	2.8 ± 0.2	7.4 ± 1.5	3.4 ± 0.4	3.3 ± 0.1	2.3 ± 0.2
Cedar	3.0 ± 0.2	8.2 ± 0.1	8.2 ± 0.3	6.2 ± 0.6	7.9 ± 0.4	4.2 ± 0.5	4.6 ± 0.1	4.4 ± 0.4	n.d.	n.d.
Bubinga	8.9 ± 0.4	7.8 ± 0.1	7.0 ± 0.2	6.5 ± 0.5	n.d.	4.7 ± 0.6	5.2 ± 0.2	4.7 ± 0.4	n.d.	n.d.
Gamma grass	6.2 ± 0.2	5.6 ± 0.2	15.8 ± 1.1	11.7 ± 0.5	7.6 ± 0.2	6.8 ± 0.5	6.9 ± 0.3	2.9 ± 0.3	n.d.	n.d.
Sugar Cane	9.8 ± 0.4	9.6 ± 0.5	11.2 ± 0.8	4.5 ± 0.3	7.7 ± 0.6	3.8 ± 0.5	4.6 ± 0.1	3.8 ± 0.5	n.d.	n.d.

Table S3. Microbially inoculated and abiotic carbon mineralized during one year incubations (char C-normalized: mgC gC⁻¹) of biochars made from different parent biomass types and combustion temperatures (as shown in Figure 2 or manuscript).

	250 °C		400 °C		525 °C		650 °C		72 hr @ 650 °C	
	biotic	abiotic	biotic	abiotic	biotic	abiotic	biotic	abiotic	biotic	abiotic
Parent										
Oak	22.5 ± 1.1	13.4 ± 1.7	20.7 ± 1.9	9.1 ± 0.7	7.8 ± 0.3	6.0 ± 1.0	8.5 ± 0.2	6.2 ± 0.6	3.6 ± 0.1	2.9 ± 0.2
Pine	29.3 ± 3.9	14.7 ± 1.5	11.2 ± 0.5	8.5 ± 0.4	8.4 ± 0.7	5.2 ± 0.4	9.1 ± 1.8	4.2 ± 0.5	4.1 ± 0.2	2.8 ± 0.2
Cedar	12.8 ± 0.3	12.4 ± 0.2	10.5 ± 0.4	8.0 ± 0.8	9.3 ± 0.5	4.9 ± 0.6	5.5 ± 0.1	5.2 ± 0.4	n.d.	n.d.
Bubinga	14.4 ± 0.7	12.7 ± 0.2	8.9 ± 0.3	8.3 ± 0.6	n.d.	5.5 ± 0.7	6.2 ± 0.3	5.6 ± 0.5	n.d.	n.d.
Gamma grass	12.5 ± 0.4	11.4 ± 0.4	30.2 ± 2	22.4 ± 0.9	15.7 ± 0.4	14.1 ± 1.1	12.5 ± 0.5	5.3 ± 0.5	n.d.	n.d.
Sugar Cane	17.4 ± 0.6	17.1 ± 0.8	18.3 ± 1.3	7.3 ± 0.5	11.7 ± 1.0	5.7 ± 0.8	6.0 ± 0.2	4.9 ± 0.7	n.d.	n.d.

Table S4. Significant relationships between biochar mineralization rate and chemical and physical characteristics of biochars

	Modeled abiotic %C _{lost} 100 y	Measured tot. min. (mgC/g char-y)	Measured tot. abiotic min. (mgC/g char-y)	S.A.-N ₂ ¹ (m ² /g)	S.A.-CO ₂ (m ² /g)	OC (wght.%)	O (wght.%)	Yield (wght.%)	Volatile matter (wght.%)	Volatile Carbon (wght.%)
Modeled %C _{lost} -100 y	0.46 ²	0.45	0.56	<u>0.24</u>	<u>0.47</u>	<u>0.49</u>	0.47	0.36	0.35	0.18
Modeled abiotic %C _{lost} -100 y		0.22	0.50	<u>0.41</u>	<u>0.30</u>	<u>0.36</u>	0.33	0.39	0.42	0.27
Measured tot. min. (mg C/g char-y)			0.55	<u>0.20</u>	<u>0.22</u>	<u>0.34</u>	0.33	n.s.	0.35	n.s.
Measured tot. abiotic min. (mg C/g char-y)				<u>0.40</u>	<u>0.18</u>	<u>0.36</u>	0.36	0.27	0.44	0.29
S.A.-N ₂ m ² /g					0.53	0.40	<u>0.37</u>	<u>0.31</u>	<u>0.48</u>	0.28
S.A.-CO ₂ m ² /g						0.51	<u>0.46</u>	<u>0.55</u>	<u>0.33</u>	n.s.
OC (wght.%)							0.99	<u>0.24</u>	<u>0.53</u>	n.s.
O (wght.%)								0.21	0.52	n.s.
Yield (wght.%)									0.29	n.s.
Volatile matter (wght.%)										0.66

1. Abbreviation same as Table S1.

2. Correlation coefficient (r^2) for linear significant (i.e. $p > 0.05$) relationship between two variables; underlined when relationship is indirect, n.s. = relationship not significant at 95% level.

Table S5. Degradation parameters for total (biotic + abiotic) mineralization

Biochar			Linear Parameters (ln <i>k</i> vs. ln <i>t</i>) ¹			Modeled Degradation Parameters				
Parent Biomass	Combust Temp	Size ²	slope	intercept	Cor. Coef. (r ²)	t _{1/2}	%C _{lost 100 y}	MRT ³ _{100 y}	%C _{lost 1 ky}	MRT ³ _{1 ky}
Bubinga	250	cs	-0.511	-4.879	0.697	1,203	14.8	1380	45.7	4472
Bubinga	400	cs	-0.520	-5.441	0.773	4,296	8.2	2532	24.8	8389
Bubinga	650	cs	-0.583	-5.594	0.905	15,558	6.1	3937	15.9	15065
Cedar	250	cs	-0.437	-4.980	0.749	733	16.3	1090	59.6	2983
Cedar	400	cs	-0.642	-5.331	0.940	23,815	7.0	3967	16.1	17382
Cedar	400	fn	-0.648	-5.253	0.948	21,770	7.5	3779	16.9	16804
Cedar	525	cs	-0.603	-5.375	0.864	12,838	7.3	3465	18.1	13878
Cedar	525	fn	-0.504	-5.231	0.863	2,283	10.6	1903	33.2	6071
Cedar	650	cs	-0.764	-6.137	0.973	2.E+07	2.7	15621	4.7	90751
Grass	250	cs	-0.313	-4.899	0.520	263	25.7	566	125.1	1163
Grass	400	cs	-0.535	-4.211	0.901	373	27.1	793	79.1	2721
Grass	525	cs	-0.521	-4.704	0.750	934	17.2	1218	51.7	4044
Grass	650	cs	-0.267	-4.683	0.124	152	36.9	370	199.3	685
Oak	250	cs	-0.574	-4.417	0.955	843	20.2	1164	53.8	4363
Oak	250	fn	-0.564	-4.330	0.858	622	22.5	1018	61.5	3726
Oak	400	cs	-0.570	-4.516	0.948	1,021	18.4	1263	49.6	4695
Oak	525	cs	-0.582	-5.398	0.879	9,592	7.4	3223	19.4	12311
Oak	525	fn	-0.808	-5.631	0.978	3.E+07	4.5	11537	7.0	74202
Oak	650	cs	-0.679	-5.513	0.901	96,169	5.5	5652	11.5	26985
Oak	650	fn	-0.591	-5.350	0.636	9,923	7.6	3205	19.6	12501
Pine	250	cs	-1.047	-4.706	0.960	a	6.7	13738	8.2	153088
Pine	400	cs	-0.456	-5.054	0.881	990	14.4	1280	50.3	3657
Pine	525	cs	-0.556	-5.419	0.753	6,786	7.7	2928	21.4	10542
Pine	525	fn	-0.519	-5.217	0.753	2,649	10.3	2011	31.3	6642
Pine	650	cs	-0.536	-5.264	0.780	3,643	9.4	2284	27.5	7856
Pine	650	fn	-0.589	-5.587	0.754	16,991	6.1	4018	15.6	15590
SugCane	250	cs	-0.486	-4.720	0.794	691	18.5	1051	60.5	3215
SugCane	400	cs	-0.662	-4.868	0.933	9,306	10.8	2740	23.5	12574

SugCane	525	cs	-0.542	-5.016	0.870	2,281	11.9	1829	34.3	6369
SugCane	650	cs	-0.647	-5.934	0.881	146,556	3.8	7430	8.6	32954
Oak	400 - 72h	cs	-0.703	-5.197	0.884	64,218	7.3	4598	14.5	23188
Oak	650 - 72h	cs	-0.747	-6.498	0.966	4.E+07	1.9	20660	3.4	115259
Pine	400 - 72h	cs	-0.656	-6.033	0.787	249,055	3.4	8558	7.5	38777
Pine	650 - 72h	cs	-0.580	-6.254	0.921	71,801	3.2	7528	8.3	28645

Notes

1. When $\ln(k)$ in units of y^{-1} and $\ln(t)$ are in units of y
 2. Cs = coarse (250-2000 μm), fn = fine (<250 μm)
 3. MRT = Instantaneous mean residence time for the time given (in y), calculated as the inverse of the degradation constant k .
- a = cannot be calculated

Table S6. Degradation parameters for abiotic mineralization

Biochar			Linear Parameters (ln k vs. ln t) ¹			Model Degradation Parameters				
Parent Biomass	Combust Temp	Size ²	slope	intercept	Cor. Coef. (r ²)	t _{1/2}	%C _{lost 100 y}	MRT ³ _{100 y}	%C _{lost 1 ky}	MRT ³ _{100 y}
Bubinga	250	cs	-0.490	-4.985	0.861	1,205	14.0	1,396	45.5	4,312
Bubinga	400	cs	-0.500	-5.138	0.675	1,818	11.7	1,705	37.1	5,395
Bubinga	525	cs	-0.600	-5.771	0.739	33,300	4.9	5,097	12.3	20,312
Bubinga	650	cs	-0.701	-5.911	0.757	671,579	3.6	9,318	7.1	46,824
Cedar	250	cs	-0.614	-5.001	0.830	5,999	10.3	2,515	25.1	10,349
Cedar	400	cs	-0.548	-5.445	0.747	6,392	7.7	2,895	21.6	10,236
Cedar	400	fn	-0.523	-5.196	0.853	2,654	10.5	2,004	31.4	6,677
Cedar	525	cs	-0.712	-5.943	0.948	1.E+06	3.4	10,115	6.7	52,124
Cedar	525	fn	-0.449	-5.477	0.404	1,996	9.6	1,889	34.2	5,310
Cedar	650	cs	-0.481	-5.678	0.741	4,183	7.2	2,677	23.8	8,098
Grass	250	cs	-0.384	-4.935	0.721	446	19.9	815	82.2	1,974
Grass	400	cs	-0.419	-4.508	0.899	280	27.5	626	104.7	1,644
Grass	525	cs	-0.710	-5.020	0.707	42,633	8.7	3,989	16.9	20,474
Grass	650	cs	-0.536	-5.637	0.492	8,045	6.5	3,305	19.0	11,341
Oak	250	cs	-0.543	-4.744	0.808	1,269	15.6	1,398	44.8	4,877
Oak	250	fn	-0.547	-4.841	0.505	1,644	14.1	1,570	39.9	5,527
Oak	400	cs	-0.458	-5.290	0.525	1,558	11.3	1,635	39.3	4,693
Oak	525	cs	-0.506	-5.564	0.534	4,592	7.6	2,681	23.5	8,597
Oak	525	fn	-0.338	-5.380	0.124	636	14.7	1,029	67.4	2,239
Oak	650	cs	-0.500	-5.691	0.485	5,514	6.7	2,967	21.3	9,394
Oak	650	fn	-0.405	-5.252	0.549	887	13.6	1,232	53.7	3,130
Pine	250	cs	-0.575	-4.845	0.487	2,323	13.1	1,792	34.9	6,730
Pine	400	cs	-0.182	-5.092	0.101	170	32.5	377	213.3	574
Pine	525	cs	-1.044	-6.694	0.739	a	0.9	98,890	1.1	1.E+06
Pine	525	fn	-0.235	-4.700	0.205	133	40.3	325	234.3	558
Pine	650	cs	-0.729	-5.829	0.939	1.E+06	3.8	9,760	7.1	52,293
Pine	650	fn	-0.618	-5.649	0.619	34,628	5.4	4,887	12.9	20,279
SugCane	250	cs	-0.426	-4.662	0.671	381	23.2	751	87.0	2,001

SugCane	400	cs	-0.494	-5.448	0.543	3,131	8.7	2,259	28.1	7,042
SugCane	525	cs	-0.709	-5.903	0.756	853,859	3.6	9,580	7.0	49,010
Oak	650-72 h	cs	-0.718	-6.683	0.903	2.E+07	1.6	21,757	3.1	113,530

Notes same as Sup. Table 3

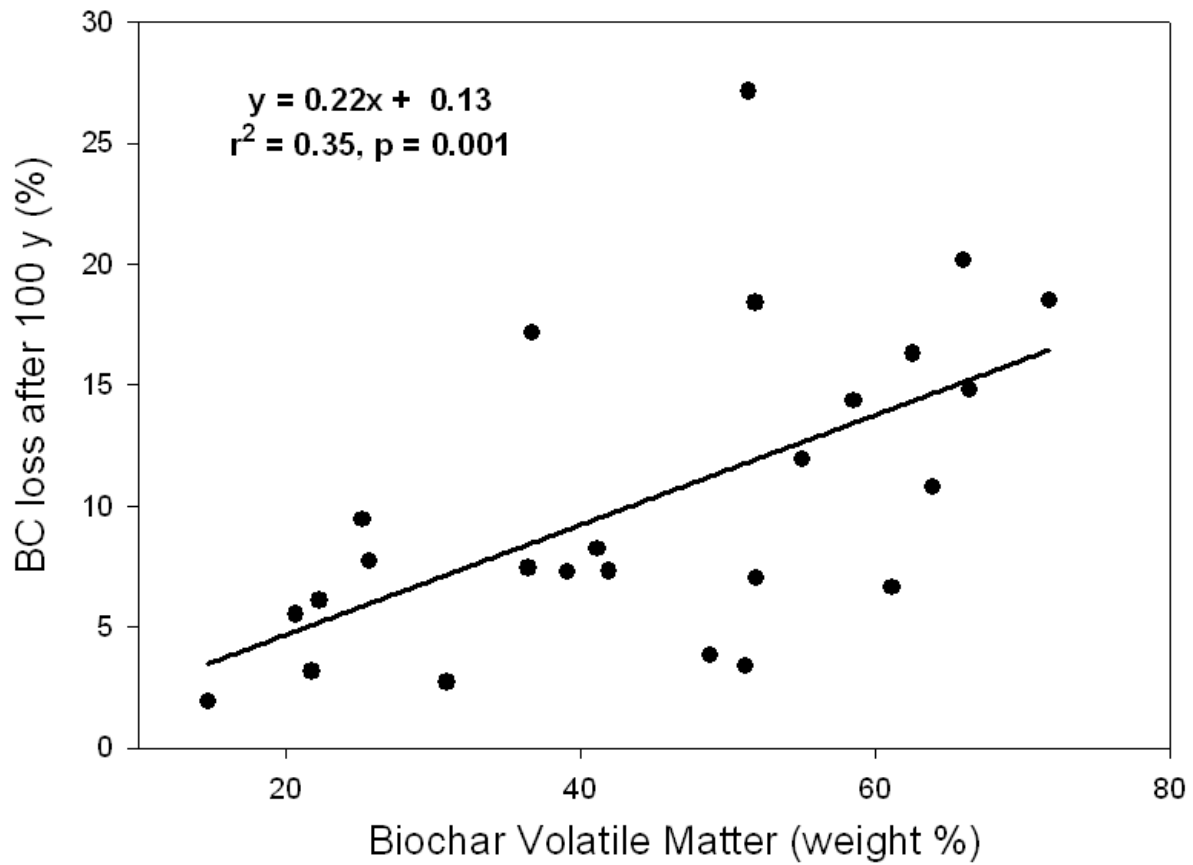


Figure S1. Linear relationship between biochar C lost after 100 y (modeled using data from of microbially-inoculated incubations of ‘coarse-grained’ biochar; 0.25-2 mm) and volatile carbon content (determined as weight loss after combustion at 850-900°C for 6 min.).